v. 2, n. 1, 2025

International Journal of
Exact
Sciences

BEYOND QUANTIFICATION: A METHODOLOGICAL DISCUSSION ON RAMAN SPECTROSCOPY FOR THICK FILMS

Acceptance date: XX/XX/2024

Helena Cristina Vasconcelos
Faculty of Science and Technology, University of the Azores, Ponta Delgada, S. Miguel, Azores, Laboratory of Instrumentation, Biomedical Engineering and Radiation Physics (LIBPhys, UNL), Department of Physics, NOVA School of Science and Technology, Caparica, Portugal

Maria Meirelles
Faculty of Science and Technology, University of the Azores, Ponta Delgada, S. Miguel, Azores, Research Institute of Marine Sciences of the University of the Azores (OKEANOS), Horta, Faial, Azores

Abstract: The characterization of crystallinity in thick films containing dispersed nanocrystals within an amorphous matrix is essential for optimizing their functional properties in applications such as optical coatings and sensors. SiO_2-TiO_2 films serve as an example of such systems, where nanocrystalline (anatase) domains coexist within an amorphous phase. The degree of crystallinity and its spatial distribution significantly influences the optical, mechanical, and electronic properties of these materials, making accurate characterization crucial for performance optimization. Raman spectroscopy is a powerful non-destructive tool for analyzing these heterogeneous materials, enabling phase identification, crystallinity quantification, and structural characterization. However, its accuracy is challenged by factors such as laser penetration depth, crystal distribution, and signal attenuation, which complicate data interpretation. Additional complexities arise from nanocrystal size variations, orientation effects, and multiple scattering, all of which must be considered for reliable analysis. This work explores the theoretical and experimental complexities of applying Raman spectroscopy to thick films, offering a critical discussion on methodological strategies for improved analysis. Key aspects such as crystallinity gradients, laser interactions, and signal deconvolution are examined to provide guidelines for refining Raman-based characterization techniques. Furthermore, the role of instrumental parameters, such as excitation wavelength, objective numerical aperture, and detection geometry, is evaluated for optimizing spectral acquisition. Experimental observations from anatase-dispersed films illustrate these challenges and serve as a basis for future methodological advancements. The discussion aims to establish best practices for the Raman analysis of thick nanocomposite films, ensuring that the measured spectra accurately represent the material's true structural characteristics.

INTRODUCTION

Crystallinity plays a crucial role in determining the physical, chemical, and mechanical properties of materials, particularly in thick films used in advanced applications such as electronic devices, solar cells, and functional coatings. The ability to quantify crystallinity is essential for optimizing material performance, as it influences properties like electrical conductivity, optical transparency, and mechanical strength. Among various characterization techniques, Raman spectroscopy has emerged as a powerful and non-destructive tool, offering high spatial resolution and the ability to differentiate between crystalline and amorphous phases [1].

Raman spectroscopy relies on inelastic light scattering, where energy shifts in the scattered photons provide information about molecular vibrations. This technique is particularly effective for crystallinity studies since Raman peak intensity and shape are highly sensitive to structural order [2]. However, several challenges arise when applying Raman spectroscopy to thick films. The signal must represent the entire film volume rather than just the surface, requiring careful consideration of laser penetration depth, internal reflections, and heterogeneous crystal distributions to ensure accurate measurements.

The intensity of the Raman signal is influenced by multiple factors, including:

1. Crystalline phase concentration: Higher crystallinity enhances Raman signal intensity.

2. Crystal size: Larger crystals exhibit stronger Raman signals due to enhanced long-range order [2]. Because of intermolecular interactions, the symmetry of a molecule in the crystalline state is generally lower than in the gaseous (isolated), but much higher than in solution and amorphous state [3].

3. Crystal arrangement: Orientation relative to the laser's electric field influences spectral features [2].

4. Multiple reflections: Light can undergo multiple internal reflections, altering the detected signal intensity.

5. Laser penetration depth: The depth of focus must be optimized to ensure signal representativeness. The laser beam remains approximately constant in diameter up to a certain distance from the focal plane, defining the beam waist (w) (Figure 1) [4].

To address these challenges, this study presents a basic methodology for the quantitative measurement of crystallinity in thick films, focusing on SiO2-TiO2 systems produced by the sol-gel method. We propose a distribution of crystallinity along the film thickness modeled by an exponential decay function, justified by factors inherent to the sol-gel method, such as oxygen access during thermal treatment, temperature gradients, and diffusion of chemical species. The laser beam waist, which determines the depth of focus, must be carefully optimized to ensure that the Raman signal is representative of the entire film volume.

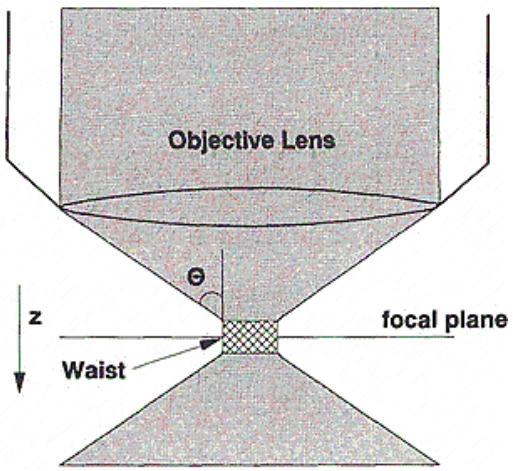

Figure 1. Laser beam distribution near the focus. From [4].

RAMAN SPECTROSCOPY: LIGHT SCATTERING AND MOLECULAR VIBRATIONS

Raman spectroscopy is an analytical technique that probes molecular vibrations, crystal structures, and chemical compositions through the interaction of light with matter. It is based on inelastic light scattering, where the energy of photons is transferred to or from molecular vibrations, producing spectral shifts characteristic of the material.

When light interacts with a material, it can excite the material to a higher energy state, known as a virtual state. This virtual state is not a stable electronic state but rather a transient, short-lived state that exists for only about one femtosecond (10^{-15} seconds). During this brief moment, the electric field of the incident light induces an oscillating electric dipole in the material. This induced dipole corresponds to a higher energy state, but it quickly re-emits energy, causing the material to return to its ground state.

The key to understanding Raman spectroscopy lies in what happens during this re-emission process. There are two primary outcomes: Rayleigh scattering and Raman scattering. In Rayleigh scattering, the material returns to its exact initial state, and the scattered photon has the same energy as the incident photon. This is an elastic scattering process, meaning there is no net change in the energy of the system.

Raman scattering, on the other hand, is an inelastic process. Here, the material does not return to its initial state but instead ends up in a different vibrational state. This leads to two possibilities: Stokes Raman scattering and Anti-Stokes Raman scattering. In Stokes scattering, the material ends up in a higher vibrational state than it started, resulting in a scattered photon with less energy than the incident photon. Conversely, in Anti-Stokes scattering, the material starts in an excited vibrational state and returns to the ground state,

emitting a photon with more energy than the incident photon.

To fully understand Raman spectroscopy, it is essential to grasp the energy landscape of the material being studied. Each molecule or material has electronic states, each with its own set of vibrational energy levels. Both the ground and excited electronic states contain a "ladder" of vibrational levels. When light interacts with the material, it can excite the system to a virtual state, an intermediate and transient state between electronic states that facilitates the scattering process.

The energy difference between the incident photon and the scattered photon corresponds to the vibrational energy of the molecule. This difference, known as the Raman shift, is measured in wavenumbers (cm^{-1}) and provides crucial information about the vibrational modes of the material, allowing the identification of specific molecular bonds and structures.

Not all vibrational modes are Raman active. For a mode to be Raman active, there must be a change in the molecule's polarizability during vibration. Polarizability refers to the ability of a molecule's electron cloud to be distorted by an external electric field, such as the oscillating field of incident light. Symmetric stretching vibrations, in which the molecule expands and contracts uniformly, often lead to significant changes in polarizability and are therefore Raman active.

In the case of silica (SiO_2) glass, Raman spectroscopy detects the symmetric stretching modes of Si–O bonds. As oxygen atoms move symmetrically, the molecule's polarizability changes, making these vibrations detectable in the Raman spectrum [3]. In contrast, asymmetric stretches or bending modes are not always Raman active, as they may not result in significant changes in polarizability. Consequently, Raman and IR spectroscopy are complementary techniques. While Raman spectroscopy depends on changes in polarizability, IR spectroscopy relies on variations in the molecule's dipole moment. In the study of silica glass, for instance, the IR spectrum may reveal asymmetric stretching modes, while the Raman spectrum highlights symmetric stretches.

Raman spectroscopy has a wide range of applications, including material identification, crystal structure analysis, and chemical composition studies [2]. It is also valuable for investigating materials with complex structures, such as glasses and amorphous solids. Unlike crystals, which have highly ordered atomic arrangements and well-defined vibrational modes, glasses exhibit a more disordered and irregular structure. In silica glass, Raman spectroscopy reveals distinct features, including a strong peak at ~800 cm^{-1} (SiO_4 tetrahedral breathing mode) and weaker bands at ~490 cm^{-1} (D1 defect mode) and ~600 cm^{-1} (D2 defect mode) [5]. These peaks help characterize the short-range order and network structure of amorphous silica, demonstrating Raman spectroscopy's ability to analyse both crystalline and amorphous materials.

RAMAN SPECTROSCOPY OF THICK SILICA-TITANIA SOL-GEL FILMS: A CASE STUDY

The study of thick films composed of mixed oxides such as SiO_2-TiO_2 is essential for applications in optical coatings, sensors, and catalysts. A key factor in these applications is the degree of crystallinity, which directly affects the material's properties and performance. SiO_2-TiO_2 films are typically synthesized using the sol-gel technique, which involves the hydrolysis and condensation of metal alkoxides, followed by spin-coating deposition and thermal densification [6-9]. This method enables precise control over composition and film thickness, which in turn influences the crystalline phase distribution and Raman spectral features.

In optical applications, such as planar waveguides for integrated optics [10-13], maintaining a highly uniform amorphous structure is crucial to minimizing optical losses. However, during thermal densification, anatase TiO_2 crystallites may precipitate from the glassy matrix, potentially degrading the optical properties of the films. The onset of anatase crystallization is strongly composition--dependent, with TiO_2-rich films (above 20 wt% TiO_2) exhibiting anatase formation after appropriate heat treatment [6].

The quantitative measurement of crystallinity in thick SiO_2-TiO_2 films using Raman spectroscopy requires a comprehensive theoretical framework that accounts for multiple factors influencing the Raman signal, including film thickness, phase distribution, and thermal history. Raman spectroscopy is particularly useful for detecting anatase TiO_2 due to its characteristic vibrational modes.

The Raman spectra of SiO_2-TiO_2 films with varying compositions ($20TiO_2$-$80SiO_2$, $30TiO_2$-$70SiO_2$, and $40TiO_2$-$60SiO_2$) and thicknesses (~1 μm and ~3 μm) are shown in Figure 2. The spectra highlight the distinct Raman peaks of anatase TiO_2, with the most intense peak at ~144 cm^{-1}, corresponding to the Eg mode of anatase. Additional anatase peaks are observed at ~123 cm^{-1} and ~197 cm^{-1}. The 144 cm^{-1} peak, associated with O-Ti-O bending vibrations, serves as a hallmark of anatase and is commonly used to quantify its phase in TiO_2-based materials [1, 14]. These spectral features provide critical insight into the crystallization behavior of TiO_2 within the SiO_2 matrix and its dependence on composition and thermal processing conditions.

The Raman spectra of the SiO2-TiO2 films shown in Figure2 revealed a strong anatase peak at ~144 cm−1, indicating the presence of crystalline TiO_2 (anatase). The peak at 123 cm-1 may be assigned to a surface phonon mode of the precipitated anatase crystals [1].

The intensity of this peak decreased with thickness, reflecting the combined effects of oxygen access, temperature gradients, and diffusion of chemical species.

These effects are closely related to the synthesis conditions and film deposition process. In order to obtain the samples studied, precursor solutions were prepared following a method similar to that described in [6], using tetraethoxysilane (TEOS) and titanium tetraisopropoxide (TPOT) (Alfa Products, 99%). Initially, TEOS was dissolved in absolute ethanol and pre-hydrolyzed at 70°C for 1 hour with a molar ratio of H_2O:TEOS=2, using hydrochloric acid (HCl) as the catalyst. Subsequently, TPOT was added to the pre-hydrolyzed solution to obtain the target composition of (100-x) SiO_2 - x TiO_2, where x = 20, 30, and 40 wt%. The SiO_2-TiO_2 films, with thicknesses of up to ~3 μm, were deposited onto silicon wafers through repeated cycles of spin-coating and thermal densification. Spin-coating was performed using a Laurell WS-400-6NPP-LITE spin coater (Laurell Technologies Corporation, USA) at 2500 rpm for 30 seconds. Each deposited layer was thermally densified at 900°C for approximately 10 seconds. Finally, the multilayer films were annealed at 1000°C for 1 hour.

Micro-Raman spectroscopy was conducted at room temperature using a system equipped with a triple monochromator (Spex model 1877), an Olympus BH2-UMA microscope, and an argon ion laser for excitation at a wavelength of 514.5 nm and the power level was typically 1W. The signal was detected in a back-scattering geometry using a Spex Spectrum One CCD detector, without polarization analysis. The accuracy of the Raman measurements is estimated to be within ±2 cm^{-1}.

The crystallized volume fraction of each SiO_2-TiO_2 film, after heat treatment, was calculated from the intensity of the anatase peak at 144 cm^{-1} (Table 1). A pure TiO_2 (anatase)

International Journal of Exact Sciences ISSN 2966-1153 DOI https://doi.org/10.22533/at.ed.153212520018

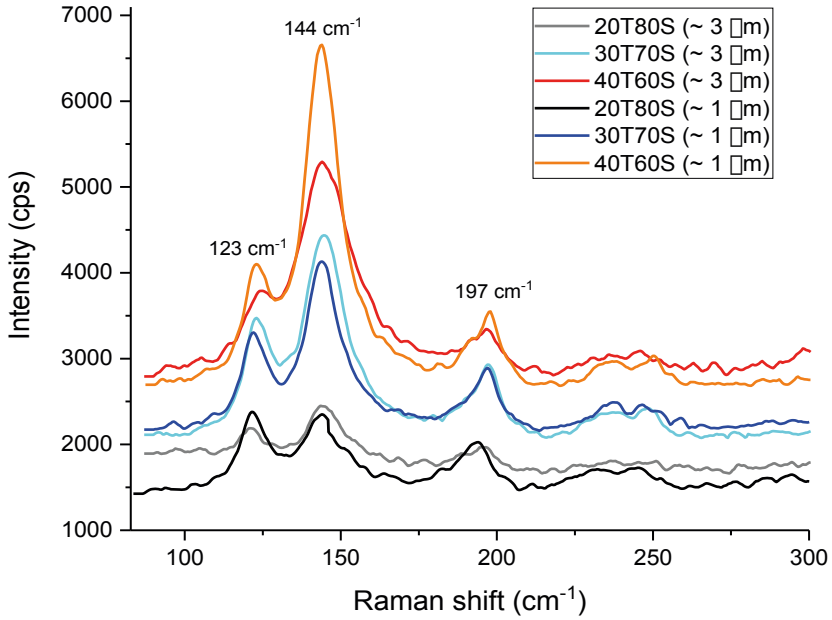

Figure 2. Raman spectra of SiO_2-TiO_2 films with different compositions ($20TiO_2$-$80SiO_2$, $30TiO_2$-$70SiO_2$, and $40TiO_2$-$60SiO_2$) and thicknesses (~1 μm and ~3 μm). The spectra show characteristic peaks of anatase (TiO_2), with the most intense peak at ~144 cm^{-1} corresponding to the Eg mode of anatase. Other anatase peaks are observed at ~123 cm^{-1} and ~197 cm^{-1}.

sample was considered as 100% crystalline [14]. Table 1 gives values of the crystallized volume fraction of anatase (V_{an}), as a function of composition (TiO_2 wt%). The intensity of the Raman shift at 144 cm^{-1} and the volume percentage of anatase, where calculated using the following equation:

$$\frac{I_{sample}}{I_{100\%\ anatase}} = V_{an}\%$$

Sample	*d* (mm)	$I_{144\ cm-1}$ (cps)	V_{an} (%)
100T	n.a.	32000	100
20T80S	1	924	3
20T80S	3	553	2
30T70S	1	2325	7
30T70S	3	1955	6
40T60S	1	3951	12
40T60S	3	2500	8

Table 1. The intensity of Raman shift at 144 cm^{-1} and volume % of anatase

Measurement Conditions**:** Laser power = 1 W, Exposure time = 50 sec, *w*~400 nm

The relationship between sample thickness, the amount of anatase crystallites, and Raman signal intensity may seem contradictory at first glance, but it becomes clearer when considering key factors. In thicker samples, the Raman signal is attenuated as the laser penetrates the material, losing energy through interactions that lead to absorption and scattering. Consequently, even if a thicker sample contains more anatase crystallites, the Raman signal may appear weaker due to this attenuation. Similarly, while the quantity of anatase crystallites influences Raman signal intensity, this effect is only significant if the laser can efficiently interact with them. In thicker samples, the signal generated in deeper layers may not reach the detector with the same intensity as that from surface layers, leading to a competition between thickness and crystallite content. If the sample is too thick, attenuation may outweigh the benefit of a higher crystallite concentration, whereas in thinner samples, reduced attenuation allows the signal to more accurately reflect the crystallite content.

Experimental observations from anatase-dispersed SiO_2-TiO_2 films highlight the challenges associated with Raman characterization of nanocomposite thick films. Variations in film thickness, composition, and heat treatment parameters all contribute to spectral differences that must be carefully analyzed. In most cases, Raman spectroscopy is used without explicitly accounting for thickness effects, assuming that the signal intensity directly corresponds to the material's crystallinity. However, the assumption that the anatase crystallite distribution follows an exponentially decreasing trend from the surface is plausible and can be mathematically modeled. This behavior is commonly observed in thin films deposited by methods such as sol-gel, where crystallization is more pronounced at the surface and gradually decreases toward the substrate.

To improve the accuracy of Raman spectroscopy in thick films, methodological adjustments can be made. One approach is to optimize the beam waist (w), where using a larger waist (e.g., 2 μm) increases laser penetration depth and enhances signal collection from deeper layers. This study aims to establish best practices for Raman spectroscopy analysis of thick nanocomposite films, ensuring that measured spectra accurately reflect the material's true structural characteristics. The proposed methodology integrates theoretical models with experimental data, providing a comprehensive framework for the quantitative analysis of crystallinity in thick films.

THEORETICAL BASIS FOR RAMAN SIGNAL ANALYSIS IN THICK FILMS

RAMAN SIGNAL AND CRYSTALLINITY IN THICK FILMS

The intensity of the Raman signal (I_R) is directly proportional to the concentration of the crystalline phase (Cc) in the material. For thick films, where crystallinity may vary along the depth (z), the total Raman signal intensity (I_R) is obtained by integrating over the film thickness (d):

$$I_R = \int_0^d I_R(z)dz$$

The crystallinity distribution along the depth can be modeled by an exponential decay function:

$$C_z(z) = C_{c0}.exp\left(-\frac{z}{\delta}\right)$$

where C_{C0} is the maximum crystalline phase concentration at the surface (z=0), and δ is the decay length, which defines how quickly crystallinity decreases with depth.

This decay is governed by factors such as oxygen access, temperature gradients, and diffusion of chemical species, which are more pronounced at the surface and diminish with depth.

FACTORS CONTROLLING CRYSTALLINITY DISTRIBUTION

OXYGEN ACCESS

Oxygen is essential for the crystallization of oxide materials such as TiO_2 (anatase or rutile). In SiO_2-TiO_2 films, the surface is directly exposed to the environment, allowing efficient oxygen access during deposition or thermal treatment. However, as depth increases (z>0), oxygen availability becomes restricted due to limited diffusion. This limits the formation of crystalline TiO_2 in deeper regions, leading to a gradual decline in crystallinity.

The decay length δ represents the characteristic depth where oxygen diffusion becomes significantly restricted, thus controlling the crystallinity gradient.

TEMPERATURE GRADIENTS

Crystallization is a thermally activated process that is strongly dependent on temperature. During thermal treatments (e.g., annealing), heat is applied externally, causing the film surface (z = 0) to become hotter, while deeper regions remain relatively less heated due to the substrate acting as a heat sink.

Since higher temperatures enhance crystallization, the surface shows a higher concentration of crystalline TiO_2. As depth increases, the temperature decreases, reducing the driving force for crystallization and leading to lower crystallinity.

DIFFUSION OF CHEMICAL SPECIES

In multicomponent films like SiO_2-TiO_2, the formation of crystalline phases depends on the diffusion of titanium ions (Ti^{4+}). Near the surface, diffusion is efficient, supporting the formation of anatase nanocrystals. However, as depth increases, the migration of Ti^{4+} slows down due to longer distances and structural barriers (e.g., grain boundaries, defects).

During heat treatment, anatase crystallites grow by incorporating Ti^{4+} from the surrounding glass matrix, leading to a gradual depletion of the amorphous TiO_2 phase in deeper layers.

CRYSTAL SIZE AND ORIENTATION

The size of the crystals (Lc) significantly affects the Raman signal intensity. Larger crystals exhibit stronger Raman signals due to enhanced long-range order and reduced defects. The relationship between crystal size and Raman intensity is given by:

$$I_R(L_c) = I_{R0} \cdot \left(\frac{L_c}{L_{c0}}\right)^3$$

where I_{R0} is the Raman intensity for a reference crystal size ($Lc0$). This cubic dependence arises from the volume scaling of the crystalline domains, emphasizing the importance of crystal size in quantitative Raman analysis.

As depth increases, if crystal growth is limited by diffusion or temperature, smaller crystals will form, leading to a reduction in Raman intensity in deeper layers.

The orientation of the crystals relative to the electric field vector (E) of the laser radiation also affects the Raman signal. The intensity depends on the angle (θ) between the crystallographic axis and the electric field:

$$I_R(\theta) = I_{R0} . cos^2(\theta)$$

This relationship is derived from the dipole radiation pattern, where Raman scattering efficiency is maximized when the crystallographic axis is aligned with the electric field vector. Well-aligned crystals result in a stronger Raman signal, whereas misaligned crystals lead to increased light scattering and multiple reflections, which complicate the Raman signal. In thick films, variations in crystal orientation with depth can cause signal attenuation, necessitating careful spectral deconvolution.

MULTIPLE INTERNAL REFLECTIONS

In thick films, the Raman signal can be significantly affected by multiple internal reflections of the laser light. Each reflection alters the detected intensity, and the total Raman intensity corrected for multiple reflections is given by:

$$I_R = \frac{I_{R0}}{1 - R}$$

where I_{R0} is the initial Raman intensity and R is the reflection coefficient of the film.

This correction ensures that the measured signal accurately represents the entire film volume, not just the surface.

INFLUENCE OF BEAM WAIST (W) AND DEPTH OF FOCUS ON RAMAN SIGNAL

DEPTH OF FOCUS AND BEAM WAIST

The depth of focus of the laser beam is determined by the beam waist (w), which defines the region where the laser remains tightly focused. The waist is given by [4]:

$$w = 6.4\left(\frac{\lambda}{2\pi}\right)\left(\frac{1}{\tan\theta}\right)^2$$

where λ is the laser wavelength (e.g., 514 nm), and θ is the angle defined by the numerical aperture (NA=sinθ), as shown in Fig.1.

The Rayleigh length (z_R) is a fundamental parameter that describes the distance over which a laser beam remains tightly focused. It is defined as the distance from the beam waist (the point where the beam has the smallest radius) where the beam radius increases by a factor of √2 [15]. The Rayleigh length is given by the formula:

$$z_R = \frac{\pi w^2}{\lambda}$$

The total depth of focus is approximately:

$$Depth\ of\ Focus\ \approx 2z_R = \frac{2\pi w^2}{\lambda}$$

This implies that a smaller waist (w) results in a shorter depth of focus, which improves resolution in depth, while a larger waist (w) increases the depth of focus, meaning the Raman signal is collected from a larger volume within the film.

INTENSITY DECAY OF RAMAN SIGNAL IN DEPTH

The Gaussian beam profile means that the Raman signal intensity decreases exponentially with depth according to:

$$I_R(z) = I_{R0}.exp\left(-\frac{z^2}{w^2}\right)$$

where I_{R0} is the Raman intensity at the focus. This equation shows that the effective sampling depth of the Raman signal is determined by the beam waist (w). If w is large, the laser interacts with deeper layers, capturing more structural information but reducing depth resolution. Conversely, if w is small, the analysis is restricted to a thinner region near the surface, improving resolution but limiting depth penetration.

The concept of effective sampling depth (z_{eff}) is crucial when considering how Raman spectroscopy captures structural information from a material at different depths. The Equation $z_{eff} = \sqrt{w^2 + \delta^2}$ describes the relationship between z_{eff} the beam waist (w), and the decay length (δ). This equation accounts for both the beam's focus, which dictates how deeply the laser penetrates the material, and the material's properties, which affect the decay of the Raman signal with depth. Understanding z_{eff} is particularly crucial for analyzing thick films or materials with depth-dependent properties, as it ensures the Raman signal is representative of the entire film thickness, not just the surface. By balancing resolution and depth penetration, this equation aids in optimizing Raman spectroscopy for comprehensive material analysis. This ensures that the Raman signal is representative of the entire film thickness.

INTEGRATED MODEL FOR TOTAL RAMAN SIGNAL INTENSITY

To account for the interactions between all factors, we integrate the contributions of crystallinity (Cc), crystal size (Lc), orientation (θ), multiple reflections (R), and laser penetration (w) into a single model for the total Raman intensity:

$$\int_0^d \frac{I_{R0}\left(\frac{L_c(z)}{L_{c0}}\right)^3 . cos^2(\theta(z)).exp\left(-\frac{z}{\delta}\right).exp\left(-\frac{z^2}{w^2}\right)}{1-R} dz$$

where $\left(\frac{L_C(z)}{L_{C0}}\right)^3$ accounts for the increase in Raman intensity with crystal size, $cos^2(\emptyset(z))$ represents the effect of crystal orientation on Raman scattering, $exp\left(-\frac{z}{\delta}\right)$, describes the crystallinity decay due to oxygen diffusion, temperature gradients, and chemical species migration, $exp\left(-\frac{z^2}{w^2}\right)$ accounts for laser intensity decay due to Gaussian focusing and $\frac{1}{1-R}$ corrects for multiple reflections within the film.

CONCLUSION

This study highlights critical aspects of Raman spectroscopy analysis in thick amorphous and crystalline films, particularly those obtained via sol-gel deposition. While the determination of crystallinity in such systems is a common practice, the influence of film thickness on the Raman signal is often overlooked. By integrating a theoretical framework with an analytical approach, this work draws attention to the limitations of conventional interpretations and underscores the need for more rigorous consideration of depth-dependent effects.

A key insight from this study is the relevance of an exponential decay model to describe the crystallinity gradient in thick films. This model suggests that the concentration of the crystalline phase (Cc) decreases with depth (z), influenced by factors such as oxygen diffusion, temperature gradients, and variations in chemical mobility during film formation. While commonly assumed to be uniform, the crystallinity distribution in such films may instead follow a depth-dependent trend, affecting the accuracy of Raman-based quantification.

REFERENCES

[1] R. M. Almeida, X. M. Du, Raman scattering from anatase nanocrystals in sol-gel derived SiO2-TiO2 glass films", CD-ROM Proceedings of the 5th European Society of Glass Science, June 21. - 24. 1999, Prague, Czech Republic

[2] A. Wang et al Applied Spectroscopy, 48 (1994) 959

[3] Nakamoto, K., Infrared and Raman Spectra of Inorganic and Coordination Compounds, 3rd Ed., John Wiley and Sons, New York, 1978

[4] Tabaksblat, R., Meier, R. J., & Kip, B. J. (1992). Confocal Raman Microspectroscopy: Theory and Application to Thin Polymer Samples. Applied Spectroscopy, 46(1), 60–68. doi:10.1366/0003702924444434

[5] Humbert, B., Burneau, A., Gallas, J. P., & Lavalley, J. C. (1992). Origin of the Raman bands, D1 and D2, in high surface area and vitreous silicas. Journal of Non-Crystalline Solids, 143, 75–83. doi:10.1016/s0022-3093(05)80555-1

[6] Strohhöfer, C., Fick, J., Vasconcelos, H. C., & Almeida, R. M. (1998). "Active optical properties of erbium nanocrystals in sol-gel derived glass films". *Journal of Non-Crystalline Solids*, 226(1-2), 182-191. https://doi.org/10.1016/S0022-3093(98)00365-2.

[7] Guglielmi, M., Martucci, A., Almeida, R. M., Vasconcelos, H. C., Yeatman, E. M., Dawnay, E. J. C., Fardad, M. A. (1998). "Spinning deposition of silica and silica-titania optical coatings: round robin test". *Journal of Materials Research*, 13(3), 731-738. https://doi.org/10.1557/JMR.1998.0092

[8] Santos, L. F., Vasconcelos, H. C., Barros Marques, M. I., Lyon, O., & Almeida, R. M. (2002). "Physical characterization of active nanocrystals in erbium-doped silica-titania nanocomposite sol-gel films". *Key Engineering Materials,* 230-232, 644-647. https://doi.org/10.4028/www.scientific.net/KEM.230-232.644.

[9] Vasconcelos, H. C., Meirelles, M., Özmenteş, R., & Korkut, A. (2025). Vacuum Ultraviolet Spectroscopic Analysis of Structural Phases in TiO2 Sol–Gel Thin Films. Coatings, 15(1), 19. https://doi.org/10.3390/coatings15010019

[10] Vasconcelos, H. C. (2020). "Optical Waveguides Based on Sol-Gel Coatings". In P. Steglich (Ed.), Waveguide Technologies in Photonics and Microwave Engineering. IntechOpen. ISBN: 978-1-83968-189-9. Retrieved from https://www.intechopen.com/online-first/optical-waveguides-based-on-sol-gel-coatings.

[11] Vasconcelos, H. C., & Silva Pinto, A. (2017). "Fluorescence Properties of Rare-Earth-Doped Sol-Gel Glasses". In U. Chandra (Ed.), Recent Applications in Sol-Gel Synthesis. IntechOpen. https://doi.org/10.5772/intechopen.68534.

[12] Almeida, R. M., Morais, P. J., & Vasconcelos, H. C. (1997). "Optical loss mechanisms in nanocomposite sol-gel planar waveguides". Proc. SPIE 3136, Sol-Gel Optics IV. https://doi.org/10.1117/12.284127

[13] Almeida, R. M., & Vasconcelos, H. C. (1997). "Sol-gel technologies in thin film fabrication for integrated optics lasers and amplifiers". *Proc. SPIE 10290, Sol-Gel and Polymer Photonic Devices: A Critical Review*, 1029009. https://doi.org/10.1117/12.279836

[14] Almeida, R.M., & Christensen, E.E. (1997). Crystallization Behavior of SiO2-TiO2 Sol-Gel Thin Films. *Journal of Sol-Gel Science and Technology, 8*, 409-413.

[15] Fowles, G. R. (1968). Introduction to modern optics. Holt, Rinehart and Winston. (Published 1975 by Dover).